Activation of Aortic Endothelial Cells by Oxidized Phospholipids: A Phosphoproteomic Analysis

Alejandro Zimman,[‡,†] Sharon S. Chen,[§,||] Evangelia Komisopoulou,[§,||] Bjoern Titz,[§,||] Roxana Martínez-Pinna,[‡] Aarya Kafi,[‡] Judith A. Berliner,[‡,⊥] and Thomas G. Graeber*,[§,||,#]

Department of Pathology and Laboratory Medicine, Crump Institute for Molecular Imaging, Department of Molecular and Medical Pharmacology, Department of Medicine, and Institute for Molecular Medicine, David Geffen School of Medicine, University of California, Los Angeles, California 90095

Previous studies have shown that oxidized products of the phospholipid PAPC (Ox-PAPC) are strong activators of aortic endothelial cells and play an important role in atherosclerosis and other inflammatory diseases. We and others have demonstrated that Ox-PAPC activates specific signaling pathways and regulates a large number of genes. Using a phosphoproteomic approach based on phosphopeptide enrichment and mass spectrometry analysis, we identified candidate changes in Ox-PAPC-induced protein phosphorylation of 228 proteins. Functional annotation of these proteins showed an enrichment of the regulation of cytoskeleton, junctional components, and tyrosine kinases, all of which may contribute to the phenotypic and molecular changes observed in endothelial cells treated with Ox-PAPC. Many changes in protein phosphorylation induced by Ox-PAPC are reported here for the first time and provide new insights into the mechanism of activation by oxidized lipids, including phosphorylation-based signal transduction.

Keywords: Oxidized phospholipid • Ox-PAPC • endothelial cell • atherosclerosis • phosphoproteomics • signal transduction • phosphatase inhibitor

Introduction

One of the major contributors to heart disease and stroke is atherosclerosis, a chronic inflammatory disease of the vessel wall characterized by lipid accumulation, entry of monocytes, cell death and, in the final stage, thrombosis caused by plaque rupture. Notably, the accumulation of phospholipid oxidation products in the subendothelial space precedes the recruitment of monocytes, an early event in atherogenesis. We have previously identified oxidized products of 1-palmitoyl-2-arachi-donoyl-*sn*-3-glycero-phosphorylcholine (Ox-PAPC) as activators of endothelial–monocyte interactions.[1] Active lipid components of Ox-PAPC are found in LDL minimally modified by oxidation, apoptotic cells,[2] and atherosclerotic lesions.[3] Tsimikas et al. reported a correlation between levels of oxidized phospholipids with the risk of artery disease,[4] which supports the role of these compounds in the initiation and progression of atherosclerosis.[5]

Expression array analysis of aortic endothelial cell culture from 12 human donors showed that Ox-PAPC regulates more than 1000 genes.[6] Inflammation, cell cycle, and coagulation were some of the functions associated with the genes regulated by Ox-PAPC. Genes regulated by Ox-PAPC and the time of their activation differ significantly from other known activators. For example, the levels of inflammatory gene induction by Ox-PAPC are increased for at least 16 h, as opposed to activators such as LPS, IL-1, and TNF (important endothelial activators) where peak induction of inflammatory genes is seen at 2 h.[7]

Specific signal transduction pathways induced by Ox-PAPC have been elucidated through hypothesis-driven experiments. For example, we showed that IL-8, an inflammatory chemokine, is induced in human aortic endothelial cells (HAECs) by Ox-PAPC through a signaling cascade involving c-Src, JAK2, and STAT3.[8] Another example is the up-regulation of tissue factor via ERK activation in human umbilical vein endothelial cell.[9] Reported changes in protein phosphorylation induced by Ox-PAPC in HAECs include c-Src, STAT3,[10] JAK2,[8] eNOS, and AKT.[11] In human pulmonary endothelial cells, Ox-PAPC induces the phosphorylation of Raf, MEK1/2, p90 RSK, Elk, MKK3/6, p38, HSP27, JNK, ATF2, MYPT1, cofillin, FAK, and paxillin.[12] Despite the progress achieved by immunoblotting-based approaches, more information is needed to identify the network of cell surface proteins and signal transduction pathways regulating the concerted response to Ox-PAPC.

Recent developments in phosphoproteomics allow a comprehensive study of protein phosphorylation and reduce the time and cost associated with antibody-based research. Mass spectrometry (MS) can identify the phosphorylation of recep-

* To whom correspondence should be addressed. E-mail, tgraeber@mednet.ucla.edu; phone, (+1) 310-206-6122; fax, (+1) 310-206-8975. Department of Molecular and Medical Pharmacology. David Geffen School of Medicine, University of California, Los Angeles, Los Angeles, CA 90095-1770.
‡ Department of Pathology and Laboratory Medicine.
† Current address: Department of Molecular Cardiology, Lerner Research Institute, Cleveland Clinic, 9500 Euclid Avenue, Cleveland, OH 44195.
§ Crump Institute for Molecular Imaging.
|| Department of Molecular and Medical Pharmacology.
⊥ Department of Medicine.
Institute for Molecular Medicine.

tors and other signaling molecules at specific amino acid residues and provides a global survey of protein phosphorylation events that can be used in system biology studies. Among the existing protocols, digestion of proteins in solution, enrichment of phosphopeptides, and identification of peptides by liquid chromatography coupled to MS allow for the determination of hundreds of phosphorylation events in a single analysis.[13−16] We have employed these techniques to identify and quantify the changes in phosphorylation induced by biologically active phospholipids in endothelial cells.

Ox-PAPC is a chronic low level activator of endothelial cells, and the magnitude of phosphorylation events induced by physiological levels of Ox-PAPC is relatively low in comparison to ligands such as growth factors. Thus, for these studies, we employed the phosphatase inhibitors vanadate and okadaic acid. These inhibitors have been successfully used to identify critical phosphorylation events stimulated by receptor activation in normal cells in cases where the increase in phosphorylation of signaling proteins contributes to downstream events but is otherwise relatively small and transient.[17−19] Many changes in protein phosphorylation induced by Ox-PAPC are presented here for the first time. We also identify specific sites of phosphorylation in proteins known to be activated by Ox-PAPC.

Methods

Cell Culture and Ox-PAPC Treatment. Bovine aortic endothelia cells (BAECs) (VEC Technologies, Rensselaer, NY) were cultured in MCDB131 (Invitrogen, Carlsbad, CA) supplemented with 15% FBS (HyClone, Logan, UT), 90 μg/mL heparin (Sigma, St. Louis, MO), and 20 μg/mL endothelial cell growth supplement (Fisher Scientific, Pittsburgh, PA). Human aortic endothelial cells (HAECs) were isolated as described previously[7] and cultured in M199 media (Invitrogen) supplemented with 20% FBS, 90 μg/mL heparin, and 20 μg/mL endothelial cell growth supplement.

PAPC (Avanti Polar Lipids, Alabaster, AL) was oxidized to Ox-PAPC by exposure to air as previously described,[3] and stored in chloroform. For treatment of BAECs and HAECs, chloroform was removed to obtain a lipid residue that was then resuspended in media to a final concentration of 40 μg/mL Ox-PAPC. For phospho-tyrosine enrichment, media used for control, and Ox-PAPC treated cells, contained 1 mM Na_3VO_4 (Sigma; a 100 mM stock solution was prepared using PBS as solvent) for the duration of the treatment (40 min). For phospho-serine/threonine enrichment, media used for control, and Ox-PAPC treated cells, contained 100 nM okadaic acid (EMD Chemicals, Gibbstown, NJ; a 200 μM stock solution was prepared using DMSO as solvent) for the duration of the treatment (40 min). In the case of phospho-serine/threonine enrichment, cells were pretreated with 100 nM okadaic acid for 1 h. Cells treated without phosphatase inhibitor for comparison were incubated with the same concentration and duration of PBS or DMSO solvents as their corresponding phosphatase inhibitor treated cells. Two batches of cells were expanded, treated, collected, and processed independently on separate days (biological replicates) for each enrichment procedure described below. Sodium pervanadate preparation and cell treatment was done as previously described.[20]

BAECs were lysed and digested with trypsin as described previously.[16] For phospho-tyrosine enrichment, the amount of

protein used for each sample was 30 mg. For phospho-serine/ threonine enrichment, the starting amount of protein was 10 mg.

Phospho-Tyrosine Enrichment. Enrichment of phospho-tyrosine peptides was done as described previously with minor modifications.[16] Lyophilized peptides were resuspended in 100 mM Tris-HCl and the pH adjusted to 7.4. Phospho-tyrosine peptides were immunoprecipitated with 4G10 antibody conjugated to agarose (Millipore, Billerica, MA) overnight at 4 °C. The following day, agarose beads were washed with 50 mM Tris-HCl, pH 7.4, three times followed by two washes with 25 mM NH_4HCO_3. Phosphopeptides were eluted with 0.1% trifluoroaceric acid (TFA) for 15 min at 37 °C, and concentrated by vacuum centrifugation. Further enrichment of phospho-tyrosine peptides was achieved using PHOS-Select Iron affinity gel (Sigma) using the manufacturer's protocol. Peptides were released from the affinity gel with 1.6% NH_3 in water. NH_3 and water were removed by vacuum centrifugation and the peptides concentrated and desalted using MonoTip C18 (GL Sciences, Torrance, CA).

Phospho-Serine/Threonine Enrichment. Lyophilized peptides were resuspended in 5 mM KH_2PO_4 (pH 2.65), 5 mM KCl, and 30% acetonitrile. Peptides were fractionated by strong cation exchange (SCX) chromatography using solid-phase extraction cartridges containing PolySULFOETHYL A (Poly LC, Columbia, MD). Collection of phosphopeptides started as soon as the SCX cartridge was loaded with peptides and continued throughout an initial wash with resuspension buffer (fraction Load and Wash; LW). The following fractions were collected with increasing concentrations of KCl in resuspension buffer. Fraction F1 was collected after elution with 17.5 mM KCl and fraction F2 was collected after elution with 70 mM KCl. Afterward, acetonitrile was evaporated by vacuum centrifugation and salts were removed by solid-phase extraction with C18 cartridges and eluted in 50% acetonitrile, 0.1% TFA. Lactic acid was then added to a final concentration of 150 mg/mL to decrease the binding of acidic unphosphorylated peptides in the next step.[21] Phosphopeptides were enriched using TiO_2 (PolyLC) for 45 min mixing constantly at room temperature. TiO_2 material was then washed with 45% acetonitrile, 0.1% TFA and the peptides were eluted with 3% NH_3 in water. NH_3 and water were removed by vacuum centrifugation and the peptides concentrated and desalted using MonoTip C18.

Mass Spectrometry and Phosphopeptide Identification by Fragmentation Spectra Sequencing. Phosphorylated peptides were analyzed by LC-MS/MS using an Eksigent autosampler coupled with Nano2DLC pump (Eksigent, Dublin, CA) and LTQ-Orbitrap (Thermo Fisher Scientific, Waltham, MA). The samples were loaded onto an analytical column (10 cm ×75 μm i.d.) packed with 5 μm Integrafrit Proteopep2 300 Å C18 (New Objective, Woburn, MA). Peptides were eluted into the mass spectrometer using a HPLC gradient of 5−40% Buffer B in 45 min followed by a quick gradient of 40−90% Buffer B in 10 min, where Buffer A contains 0.1% formic acid in water and Buffer B contains 0.1% formic acid in acetonitrile. All HPLC solvents were Ultima Gold quality (Fisher Scientific). Mass spectra were collected in positive ion mode using the Orbitrap for parent mass determination and the LTQ for data dependent MS/MS acquisition of the top 5 most abundant peptides. Each sample was analyzed twice (replicate runs), and in each run, one-sixth of the sample was injected. Thus, only one-third of the sample was used (10 mg of lysate protein equivalents for phospho-tyrosine enrichment and 3.3 mg for phospho-serine/

threonine enrichment). MS/MS fragmentation spectra were searched using SEQUEST (Version v.27, rev. 12, Thermo Fisher Scientific) against a bovine IPI protein database (v.3.35, released 25th September 2008 and downloaded from ftp.ebi.ac.uk). Search parameters included carboxyamidomethylation of cysteine as static modification. Dynamic modifications included phosphorylation on serine, threonine, tyrosine, and oxidation on methionine. Results derived from database searching were filtered using the following criteria: XCorr 1.0(+1), 1.5(+2), 2(+3), peptide probability score (BioWorks 3.2, Thermo Fisher Scientific) 0.001, and delta Cn 0.1. An additional filter of measured peptide mass tolerance, or mass accuracy (parts per million, ppm), was used in conjunction with both forward and reverse database searches (IPI bovine v3.35 reversed using BioWorks) to keep the false discovery rate (FDR) below 2%. The FDR was calculated as $2(n_{rev}/(n_{rev} + n_{for}))$ where n_{for} is the number of unique peptides identified from the forward database and n_{rev} is the number of unique peptide identified from a reversed database. The final FDR was 1.6% and all identified peptide mass accuracies are below 3 ppm as reported in Supplemental Tables 1 and 2. The Ascore algorithm was used to more accurately localize the phosphate on the peptide (http://ascore.med.harvard.edu).[22] An Ascore value ≥ 19 indicates that the phosphorylation site on the peptide is located with >99% certainty.

Chromatography Profile Alignment and Alignment-Based Peak Identification. As is common in data-dependent MS2 fragmentation sequencing, some peptides identified by sequencing in one sample may not be sequenced or identified in another sample even if the peak is present. Phosphopeptide peaks sequenced in some samples but not others were located in the remaining samples by aligning the chromatogram elution profiles using a dynamic time warping algorithm.[23] Several related versions and applications of chromatography alignment algorithms have also been published.[24−28] An extended explanation of the strategy, and performance results, can be found in the Supplemental Figure 1. Alignment results for each phosphopeptide peak were visually inspected across all samples using chromatography plots like those shown in Supplemental Figure 1g and 1i. Peptides with poor chromatography were eliminated from further analysis.

Quantitation of Phosphorylation Responses Activated by Ox-PAPC. Ratios of phosphopeptide peak intensities were calculated by dividing the average peak intensity from Ox-PAPC-treated cells by the average peak intensity from Control-treated cells. Peak intensities of phosphopeptides eluting in more than one fraction were added together. Each phosphopeptide peak intensity was visually inspected and corrected when necessary. In addition, a t test p-value was calculated between the replicate runs of LC-MS analysis of Control and Ox-PAPC samples. If a phosphopeptide was quantified in two biological replicates, then the lowest ratio and the maximum t test p-value value of the pair of biological replicates was selected. If the ratios of two biological replicates had opposing trends, then we assigned a ratio of 1 with no t test p-value. The vast majority of these cases involved small changes close to 1. If a phosphopeptide was quantified in only one biological replicate, then we used the single ratio and t test p-value available.

We determined the chance of obtaining a false positive result by comparing normalized values from the same treatment between biological replicates (i.e., Control vs Control and Ox-PAPC vs Ox-PAPC). The intensity values for the same phos-

phopeptide were scaled to each other by setting the mean of each peptide across the samples for one experimental batch equal to the mean for that peptide in the second experimental batch. We then established cutoff thresholds for ratio and t test p-value so that the false positive rate in our final results is less than 1%. These cutoff values were calculated independently for phosphopeptides detected and quantified in either one or two biological replicates. Phosphopeptides with the same sequence but different charge states or methionine oxidation states had to have all of the states above cutoff values to be considered as induced by Ox-PAPC.

Bovine IPI sequences were sequence-aligned using Blast against the human IPI protein sequence database (v.3.56, released 3rd March 2009; $1e^{-45}$ maximum e-value) to conduct further data analysis using the human homologue, including the identification of the corresponding phosphorylation site.

Pathway Enrichment Analysis. Pathway enrichment analysis for gene ontology (GO) terms and Kyoto Encyclopedia of Genes and Genomes (KEGG) pathway annotations were done using DAVID Bioinformatic Resources 2008 after mapping IPI proteins to Entrez genes.[29] Two groups of gene products were used to calculate enrichment p-values for the GO and KEGG functional categories: (a) "changed" is the list of proteins with significant differences in phosphorylation between Control and Ox-PAPC samples in at least one phosphorylation site as indicated in Supplemental Tables 1 and 2, and (b) "detected" is the complete list of proteins identified by mass spectrometry in the study using either phosphopeptide enrichment procedure as listed in Supplemental Tables 1 and 2. For the results summarized in Table 3 (and more completely shown in Supplemental Tables 3 and 4), we used "changed" as the gene product list and "detected" as the background list to ask whether the phosphoproteins that are modulated by Ox-PAPC exposure are functionally and statistically distinct from the background of phosphoproteins detected in our experiments. Additional pathway enrichment analysis was also done to compare the types of phosphorylated proteins detected in aortic endothelial cells compared to all proteins encoded in the genome. This analysis is fully described in Supplemental Tables 3 and 4 along with the results.

Quantitative Immunoblotting. BAECs and HAECs were lysed with 50 mM Tris-HCl (pH 7.4), 1% NP-40, 0.25% sodium deoxycholate, 150 mM NaCl, 1 mM EDTA, 1 mM PMSF, 1 μg/mL aprotinin, 1 μg/mL leupeptin, 1 μg/mL pepstatin, 1 mM Na_3VO_4, and 1 mM NaF. Protein concentration was determined using the BCA assay (Thermo Fisher Scientific). Equal amounts of proteins from each sample were loaded into the gel for electrophoresis. Proteins were then transferred to PVDF membranes and probed with mouse phospho-tyrosine (P-Tyr-100), rabbit phospho-(Ser) PKC substrate, rabbit phospho-ERK1/2 (Thr202/Tyr204), or rabbit ERK1/2 antibody (Cell Signaling, Danvers, MA). Rabbit TIE1 antibody (Santa Cruz Biotechnologies, Santa Cruz, CA) and rabbit Calnexin (Assay Designs, Ann Arbor, MI) were also used for immunoblotting. Protein and phosphoprotein levels were determined using quantitative chemiluminescence measurements on a VersaDoc Imaging System Model 5000 or a ChemiDoc XRS (Bio-Rad, Hercules, CA). For MLC2 immunoblotting, the same procedure was used except that BAECs were lysed in 8 M urea, 50 mM Tris-HCl (pH 7.4), 1 mM Na_3VO_4, and 1 mM NaF. Antibodies used were rabbit phospho-MLC2 (Thr18/Ser19), and rabbit MLC2 (Cell Signaling).

Results

Phosphatase Inhibitor Cotreatment Facilitates the Detection of Phosphorylation Changes. Our preliminary studies and published results indicated that phosphorylation induced by Ox-PAPC begins as early as 1 min after treatment and can be transient but is often prolonged and follows a different time-courses for each protein. We selected 40 min of incubation time with Ox-PAPC after a survey of published reports that indicated a large number of phosphorylation events induced by Ox-PAPC peak between 30 min and 1 h.[8,10-12] In our preliminary MS phosphoprofiling studies of Ox-PAPC-induced signaling performed in the absence of phosphatase inhibitors, we identified a large number of candidate phosphorylation events with relatively small inductions in response to Ox-PAPC. These studies convinced us that, in the absence of phosphatase inhibitors, it would not be feasible to collect enough samples, using the large number of primary endothelial cells required, to obtain statistically significant results. We reasoned that, by blocking phosphatase activity with inhibitors, we would effectively integrate the kinase-activated signaling events occurring during the first 40 min of treatment and thus result in more phosphorylation candidates.

Immunoblot analysis of global protein phosphorylation confirmed that differences between Control and Ox-PAPC were more apparent when phosphatase inhibitors were employed (Figure 1A,B, lanes 1 and 2 compared to 5 and 6). We also observed that the pattern of proteins phosphorylated was different after treatment with Ox-PAPC compared to VEGF-A or TNF-α treatment (Figure 1A,B, lanes 3, 4, 7 and 8) indicating that each ligand induces changes in phosphorylation of a different set of proteins. These differences between activators were generally smaller in the absence of phosphatase inhibitor. We further demonstrated that the inhibitory properties of vanadate are distinct and less severe than pervanadate by comparing the effect of vanadate and pervanadate on the tyrosine phosphorylation of untreated and Ox-PAPC treated cells (Figure 2). For this study, we monitored phosphorylation of ERK1/2, a protein we have previously shown to be phosphorylated in response to Ox-PAPC. Ox-PAPC induced the phosphorylation of ERK1/2 with, or without, 1 mM vanadate. On the other hand, cotreatment with 1 mM pervanadate increased the levels of ERK1/2 phosphorylation >100-fold obscuring the effect of Ox-PAPC. A similar result was seen using a pan-specific phospho-tyrosine antibody (data not shown). This result confirms that, under the experimental conditions used in our study, vanadate by itself is not causing saturation of sites of tyrosine phosphorylation as seen with pervanadate.[20] On the basis of the above studies, we chose to use these inhibitors to identify candidate Ox-PAPC-induced phosphorylation events in our global profiling studies.

Total Phosphorylation Sites Identified in Aortic Endothelial Cells. The phosphoproteomic method used in this study is based on the enrichment of phosphopeptides followed by identification and quantitation by mass spectrometry (Figure 3). We used two separate enrichment procedures to increase the detection of phosphorylation events induced by Ox-PAPC: (1) immunoprecipitation of peptides containing phosphotyrosine using a pan-specific anti-phosphotyrosine antibody, and (2) fractionation of peptides by strong cation exchange (SCX) prior to enrichment of phospho-serine/threonine peptides with TiO$_2$ metal affinity. Enrichment of tyrosine phosphorylated peptides using an anti-phosphotyrosine antibody resulted in the identification of 112 unique phosphorylation sites from 80
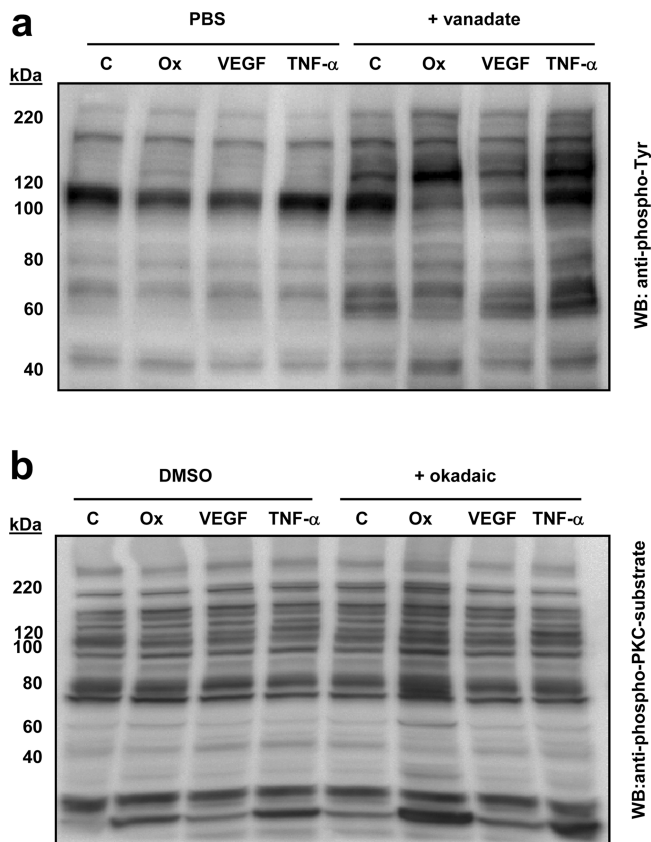

Figure 1. Phosphatase inhibitor cotreatment increases the detection of phosphorylation events induced by Ox-PAPC, VEGF-A, and TNF-α, and demonstrates distinct effects of the three activators. (a) BAECs were incubated with 40 μg/mL Ox-PAPC (Ox), 50 ng/mL VEGF-A (VEGF), 2 ng/mL TNF-α (TNF-α), or media alone (C) for 40 min in the presence, or absence, of 1 mM vanadate. Immunoblots were probed for phospho-tyrosine using a pan-specific anti-phosphotyrosine antibody. (b) BAECs were preincubated with, or without, 100 nM okadaic acid for 1 h before incubation with 40 μg/mL Ox-PAPC (Ox), 50 ng/mL VEGF-A (VEGF), 2 ng/mL TNF-α (TNF-α), or media alone (C) for 40 min. Immunoblots were probed for an antibody capable of detecting phospho-Ser PKC substrates as an indicator of changes in serine and threonine phosphorylation. The appropriate control solvent (PBS or DMSO) was included in the samples not exposed to phosphatase inhibitors as indicated.

proteins. Enrichment of serine/threonine phosphorylated peptides resulted in the identification of 831 unique phosphorylation sites from 485 proteins. All 943 phospho-tyrosine/serine/threonine peptides identified are listed in Supplemental Tables 1 and 2.

For the phospho-serine/threonine peptides enrichment protocol, we first used solid phase extraction containing SCX resin to divide the phosphoproteome in three fractions and then enriched for phosphopeptides by TiO$_2$ metal affinity. The characteristics of the phosphopeptides found in each fraction were consistent with the fractionation affinity properties of the corresponding step in the method. Similar to SCX-HPLC,[30] phosphopeptides elute based on their solution charge state calculated at the buffer pH (Supplemental Figure 2). The number of phosphopeptides found in the three SCX fractions was similar (Figure 4) and 81% of the phosphopeptides eluted in a single fraction. Almost all the overlap occurred in the first two fractions (gray bar in Figure 4). After enrichment with TiO$_2$,
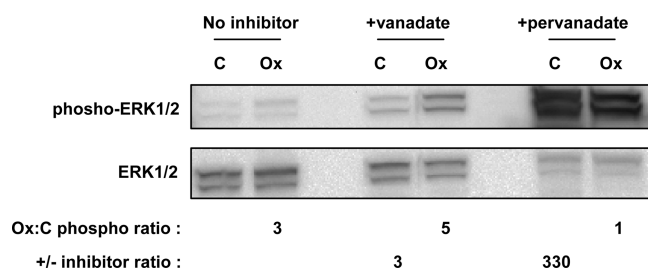
	No inhibitor		+vanadate		+pervanadate	
	C	Ox	C	Ox	C	Ox
phospho-ERK1/2						
ERK1/2						
Ox:C phospho ratio :	3		5		1	
+/- inhibitor ratio :			3		330	

Figure 2. ERK 1/2 phosphorylation induced by Ox-PAPC shows similar trends in the absence or presence of vanadate, but is masked by treatment with pervanadate. BAECs were incubated with 40 μg/mL Ox-PAPC (Ox) or media alone (C) for 40 min. Media used for the duration of the experiment (40 min) contained 1 mM vanadate, 1 mM pervanadate, or no inhibitor. Immunoblots were probed using an antibody to detect ERK 1/2 phosphorylation (Thr202/Tyr204 or Thr185/Tyr187) (top). The blot was then reprobed with an antibody to detect total levels of ERK 1/2 for normalization (middle). The increase in phosphorylation induced by Ox-PAPC was determined by quantitative chemiluminescence and expressed as fold increase compared to cells treated with media alone (Ox:C phospho ratio). The increase in phosphorylation induced by phosphatase inhibitor is expressed as fold increase compared to cells treated with no inhibitor (±inhibitor ratio).

the percentage of fragmentation sequenced peptides containing a phosphorylated residue was 97% in the first two eluting fractions, and 51% for the third fraction (Supplemental Figure 3). Eighty-nine percent of phosphopeptides enriched by SCX-TiO$_2$ had only 1 phosphate group, with 10% containing 2 phosphates (Supplemental Figure 4). In the phosphotyrosine enrichment experiments, the percentage of sequenced peptides containing a phosphorylated residue was 88%.

371 Phosphorylation Sites Induced or Repressed by Ox-PAPC. We observed 371 unique phosphorylation sites (65 phosphotyrosine, 236 phosphoserine, and 70 phosphothreonine) on 228 proteins that changed upon activation of endothelial cells with Ox-PAPC. Tables 1 and 2 list the proteins with the largest changes in phosphorylation induced by Ox-PAPC. The complete list of phosphopeptide quantitation can be found in Supplemental Tables 1 and 2. The methods described and characterized above to enrich for phospho-tyrosine and phospho-serine/threonine peptides provided consistent results between two biological replicates (Figure 5) and comparisons between biological replicates allowed us to establish ratio and t test p-value thresholds that yield false positive rates of less than 1% (see Methods and Supplemental Figure 5).

Validation of the Phosphoproteomic Results. A number of phosphorylation events in tyrosine, serine, and threonine residues induced by Ox-PAPC reported in this study were either confirmed by us using phospho-specific antibodies or previously observed by others in bovine or human endothelial cells. Using bovine cells, we validated the Ox-PAPC induced phosphorylation of two molecules, ERK1/2 and myosin light chain 2 (or myosin regulatory light chain 12B; MLC2/MRLC2/ MYL12B). We chose these molecules because antibodies were available against the specific phosphorylation event detected by mass spectrometry and because the Ox-PAPC-induced ratio in phosphorylation was substantial. ERK1/2 has been shown to play an important role in Ox-PAPC action. Ox-PAPC induced ERK1/2 phosphorylation at Thr202/Tyr204 (or Thr185/Tyr187) detected in BAECs (Figure 2) was also shown in HAECs,[31] and HUVEC[9] in the absence of vanadate. MLC2 was previously

shown not to be phosphorylated by low concentrations of Ox-PAPC but may be an important regulator of cytoskeletal changes induced by oxidized phospholipids at higher concentrations. Validation of MLC2 phosphorylation at Thr18/Ser19 was done with, and without, okadaic acid (Figure 6). Ox-PAPC increased the absolute levels of phosphorylation of MLC2, the total amounts of MLC2, and the phosphorylation per unit of MLC2 in the presence or absence of okadaic. As this example illustrates, the induced phosphorylation levels reported in Supplemental Tables 1 and 2 may in some cases be a combined effect of Ox-PAPC-induced protein levels and phosphorylation rates. We also validated the role of TIE1 receptor phosphorylation and signaling in the Ox-PAPC endothelial response. The TIE1 experiments are described below at the end of the functional significance section and in Figure 7.

Furthermore, our results confirm several Ox-PAPC-induced phosphorylation sites previously reported in the literature by Western blotting in the absence of phosphatase inhibitor. Our results corroborate the phosphorylation of human paxillin at Ser272[32] (Ser302 in BAECs), eNOS at Ser1177,[11] caveolin-1 at Tyr14,[33] and HSP27[12] induced by Ox-PAPC. Two phosphorylation sites, paxillin at Tyr118[32] and STAT3 at Tyr705,[8] previously reported in the literature to be phosphorylated upon Ox-PAPC activation were also detected in our study but without a significant change in phosphorylation. Taken together these results, and the validations of ERK1/2 and MLC2 (Figures 2 and 6), indicate a strong overlap between inhibitor-free and inhibitor-present results considering that most of the phosphorylations observed on Western blots were performed with either different doses of Ox-PAPC, in a different cell species or type, or at a different time of treatment.

We also identified novel sites of phosphorylation of proteins known to be activated by Ox-PAPC. For example, we report here phosphorylation of STAT3 at Thr714/Ser727, JAK2 at Tyr570, and VEGFR2 at Tyr1214. Previous reports show that Ox-PAPC induces the phosphorylation of STAT3 at Tyr705, JAK2 at Tyr1007/1008,[8] and VEGFR2 at Tyr1175.[31] Many other such examples exist, and a number of them are shown in Tables 4 and 5 and Supplemental Table 5. These previous studies provide further evidence that the candidates identified by MS phospho-profiling using cells stimulated in the presence of vanadate and okadaic acid include phosphorylation events that are induced even in the absence of inhibitor.

Biological Significance of the Individual Phosphorylation Events Induced by Ox-PAPC in Aortic Endothelial Cells for Atherosclerosis. We report here for the first time a large number of changes in phosphorylation upon incubation of endothelial cells with Ox-PAPC. These data provide new information important to an understanding of Ox-PAPC action that may define mechanisms of endothelial cell activation during the early stages of atherosclerosis and other inflammatory diseases that involve oxidized phospholipids. Several of the proteins with a change in phosphorylation in response to Ox-PAPC (Tables 1 and 2 and Supplemental Tables 1 and 2) may help to explain the regulation of important effects of Ox-PAPC. Though we are unable to discuss the importance of all of these newly identified phosphorylations, we cite several examples.

We have known for 10 years that the binding of monocytes to endothelial cells depends on the activation of $\alpha 5 \beta 1$ integrin, leading to the binding of CS-1 fibronectin to the apical surface of the endothelium.[34] However, the mechanism controlling this activation was not identified. The activation of $\beta 1$ integrin is a complex process with formation of several different protein
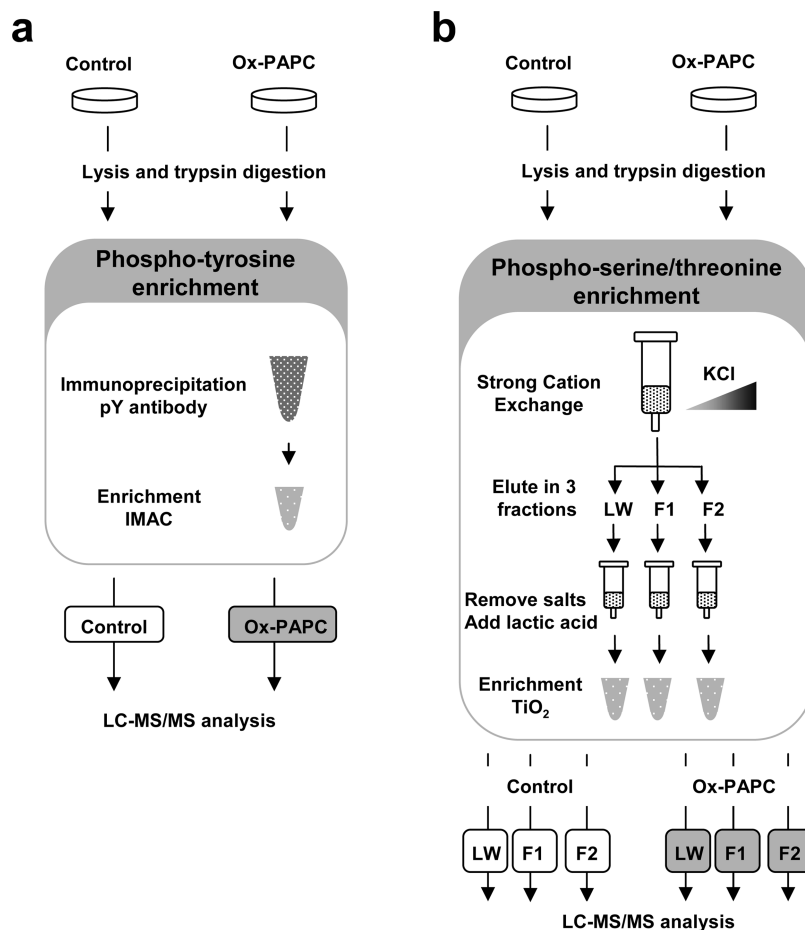
Figure 3. Experimental scheme of the phosphoproteomic enrichment methods. BAECs were treated with media alone (Control) or 40 μg/mL of Ox-PAPC for 40 min. After cell lysis and digestion of proteins with trypsin, phosphopeptides were enriched. (a) For phospho-tyrosine peptides, samples were immunoprecipitated with 4G10 antibody followed by metal affinity enrichment (IMAC). (b) For phospho-serine/threonine peptides, samples were divided in three fractions based on their binding to a strong cation exchange (SCX) cartridge. Fraction LW was collected while the peptides were loaded into the cartridge and during an initial wash with buffer containing 5 mM KCl. Fraction F1 was collected with buffer containing 17.5 mM KCl, and fraction F2 with 70 mM KCl. After salt removal, each of the fractions was further enriched for phosphopeptides using TiO$_2$ metal affinity in the presence of lactic acid. Each sample was analyzed by LC-MS/MS for peptide identification and quantitation.
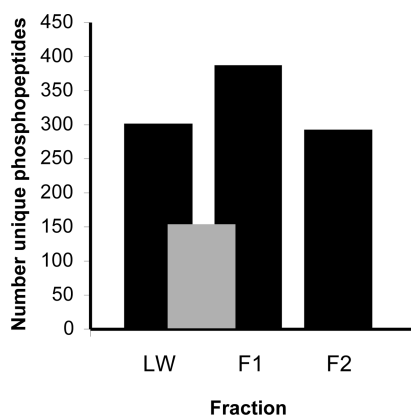

Figure 4. Number of unique phosphopeptides found in each fraction of the strong cation exchange (SCX) chromatography. Peptides were separated by solid-phase extraction-SCX chromatography prior to an enrichment of phosphopeptides by TiO$_2$ metal affinity. Black bars indicate the number of phosphopeptides found in each fraction after LC-MS/MS analysis. Gray bars indicate common phosphopeptides found between two fractions. The number of unique phosphopeptides is calculated after eliminating sequences that differ only in ion charge and oxidation of methionine.

complexes. The finding in the current study showing that Tyr783 of the β1 integrin is highly phosphorylated in response to Ox-PAPC (Table 1) suggests a mechanism that might control the β1 integrin/fibronectin axis. Phosphorylation of β1 integrin at Tyr783 favors the dissociation of the integrin—talin complex and promotes the association of integrin with tensin leading to a strengthening of the binding to fibrillar matrix molecules like fibronectin.[35]

Another novel effect of phospholipid oxidation products is their prolonged activation of several signaling pathways as compared to LPS and TNF.[7] There are many possible mechanisms by which these signals might be prolonged. However, a mechanism we had not considered is suggested by the strong phosphorylation of SHC1 at Tyr 428 (Tyr317 in some isoforms) induced by Ox-PAPC. This phosphorylation was previously shown to control the interaction of SHC1 with GRB2 and mediates the activation of Ras and Rac-1. We have previously published studies showing the sustained and important role of both Ras and Rac-1 activation in the actions of Ox-PAPC.[36,37] The potential importance of SHC1 phosphorylation in vivo is shown by the observation that the phosphorylation of two other tyrosine residues of SHC1, that also participate in GRB2

Table 1. Partial List of Phosphorylation Events Induced by Ox-PAPC Identified Using a Pan-Specific Anti-Phosphotyrosine Antibody to Enrich Phosphopeptides[a]

		bovine			human (by blast search)[b]			
	Entrez	tryptic phosphopeptide sequence[c]	phosphosite	ratio (Ox/C)	IPI	Entrez name	phosphosite sequence[c]	phosphosite
1	ITGB1	WDTGENPIyK	Y783	9.5	IPI00217563.4	integrin, beta 1	AKWDTGENPIyKSAVTTVVNP	Y783
2	VIM	TySLGSALRPTTSR	Y38	1.8	IPI00418471.6	vimentin	RSYVTTSTRTySLGSALRPST	Y38
		TLYTSSPGGVyATR	Y61	1.8			SLYASSPGGVyATRSSAVRLR	Y61
		FANyIDKVR	Y117	1.6			LQELNDRFANyIDKVRFLEQQ	Y117
		TLYTSsPGGVyATR	S56, Y61	6.4			PSTSRSLYASsPGGVyATRSSAVRLR	S56, Y61
3	CTNND1	FSDLSLNGPQDHSHLLySTVPR	Y96	5.7	IPI00182469.3	catenin, delta 1	NGPQDHSHLLySTIPRMQEPG	Y96
		SLDNNySTLNER	Y898	2.2			GSNTKSLDNNySTPNERGDHN	Y898
4	SEPT2	IYHLPDAEsDEDEDFKEQTR	S218	5.4	IPI00871851.2	septin 2	IKIYHLPDAEsDEDEDFKEQT	S253
5	AFAP1L2	SSSSDEEYIyM*NK	Y56	5.1	IPI00181905.3	actin filament associated protein 1-like 2	KSSSSDEEYIyMNKVTINKQQ	Y56
		AAQQPLSLLGCEVVPDPSPDHLySFR	Y413	3.7			VVPDPSPDHLySFRILHKGEE	Y413
6	SHC1	ELFDDPSyVNVQNLDK	Y428	5.1	IPI00021326.4	SHC transforming protein 1	AGRELFDDPSyVNVQNLDKAR	Y428

[a] All events shown here have statistically significant induction. The complete list with all significant events and further details is shown in Supplemental Table 1. [b] Human IPI, Entrez name, and phosphosite sequence are calculated by sequence alignment using Blast. [c] Phosphorylation at tyrosine, serine, or threonine is indicated by lower case "y", "s", or "t".

activation, are chronically observed in the athero-susceptible areas of the aorta.[38] These studies suggest that SHC1 may be an important candidate for the sustained regulation of several Ox-PAPC induced pathways and our results offer phosphorylation of Tyr428 as a candidate starting point for further mechanistic studies.

Finally, while the cytoskeletal changes elicited by Ox-PAPC have focused on regulation of microfilaments, our data demonstrating multiple phosphorylation sites of vimentin (Table 1 and 2), a major intermediate filament protein, and ARHGEF2 (Table 2), a regulator of microtubule structure, suggest that these cytoskeletal components may also play an important role in the effects of Ox-PAPC.

Functional Significance of the Proteins Phosphorylated upon Ox-PAPC Activation. We also conducted functional analysis of proteins with Ox-PAPC-induced phosphorylation to identify important pathways of Ox-PAPC action. We used pathway (KEGG) and gene ontology (GO) enrichment analysis to identify pathways significantly modulated by treatment of cells with Ox-PAPC. Some of the KEGG pathways with the highest enrichment values for induced phosphorylation are shown in Table 3 and the complete list is in Supplemental Table 3. These include gene products regulating the actin cytoskeleton, adherens junctions, and focal adhesions. The large number of molecules in these pathways with observed phosphorylation changes suggests a major change in cell−cell interaction as well as cell matrix interaction mediated by Ox-PAPC. This result also suggests that Ox-PAPC modulates endothelial barrier function and endothelial cell migration. These pathways control the homeostasis and activation (or dysfunction) of the endothelium.[39] Birukova et al. showed that Ox-PAPC at 20 μg/mL increases endothelial barrier protection while noting that higher concentrations disrupt barrier function by modifying the interaction between adherens junction and focal adhesion in pulmonary endothelial cells.[40,41] Our phosphorylation studies employed a concentration of 40 μg/mL, within the range expected to disrupt barrier function. In our study, we identified new sites of phosphorylation induced by Ox-PAPC that could regulate actin cytoskeleton and we confirmed others previously reported (Table 4). Two focal adhesion

proteins, zyxin and β4 integrin (Supplemental Table 5), are new candidates for major modifiers of the endothelial barrier and endothelial migration during Ox-PAPC activation based on their previously characterized functions. Zyxin is recruited to focal adhesion areas and it is essential in the formation of stress fibers in the activation of endothelial cells by thrombin, an inflammatory agent that increases endothelial barrier permeability.[42] β4 Integrin is required in endothelial cell migration.[43] Our results provide candidate proteins whose phosphorylation can be compared between Ox-PAPC treatments of 20 and 40 μg/mL in order to identify critical molecules involved in the breakdown of endothelial junction integrity.

GO terms also indicate important leads to understanding mechanisms of activation and regulation by Ox-PAPC (Table 3 and Supplemental Table 4). Prostaglandin E2 receptor subtype 2 (EP2) has been fully characterized as an Ox-PAPC-binding protein that initiates signaling pathways in endothelial cells.[44] However, other initiators of signal transduction may be possible since EP2 does not account for the activation of many of the events initiated by Ox-PAPC such as the induction of IL-8 (an inflammatory chemokine). Among the GO terms enriched by Ox-PAPC is 'protein kinase activity' which includes many Ox-PAPC-induced phosphorylations on kinases that were previously unknown (Table 5). This group of phosphorylated proteins includes receptor proteins capable of initiating cell activation through different ligands such as Vascular Endothelial Growth Factor Receptor 2 (KDR/VEGFR2), Ephrin type-A receptor 2 and 5 (EPHA2, EPHA5), and Tyrosine-protein kinase receptor TIE1 (TIE1).

On the basis of initial leads from our phosphorylation profiling, we have validated that VEGFR2 plays a key role in the activation of human aortic endothelial cells by Ox-PAPC.[31] VEGFR2 mediates SREBP and ERK1/2 activation, which leads to the upregulation of IL-8, LDL receptor, and TF (a coagulant factor) mRNA. We previously demonstrated that Ox-PAPC increases the phosphorylation at Tyr1175 and here we show that Tyr1214 is also phosphorylated. The phosphorylation of each residue leads to different downstream targets and different biological responses in the endothelial cell.[45]

Table 2. Partial List of Phosphorylation Events Induced by Ox-PAPC Identified Using Fractionation of Peptides by SCX Followed by Enrichment of Phosphopeptides by TiO$_2$ Metal Affinity to Enrich Phosphopeptides[a]

	Entrez	bovine			IPI	Entrez name	human (by blast search)[b]	
		tryptic phosphopeptide sequence[c]	phosphosite	ratio (Ox/C)			phosphosite sequence[b]	phosphosite
1	CSRP1	GYGYGQGAGtLSMDKGESLGIR GEGEGOGAGALVHsE	T79 S192	33 1.7	IPI00442073.5	cysteine and glycine-rich protein 1	KGYGYGQGAGtLSTDKGESLG FGQGAGALVHsE	T79 S192
2	VIM	TYSLGSALRPTTsR ISLPLPNFSsLNLR TYsLGsALRPTTSR IsLPLPNFSsLNLR ETNLDsLPLVDtHSKR	S49 S420 S39, S42 S412, S419 S430, T436	3.3 3.4 16.8 4.5 23.5	IPI00418471.6	Vimentin	SLGSALRPSTsRSLYASSPGG RISLPLPNFSsLNLRETNLDS SYVTTSTRTYsLGsALRPSTSRSL KLLEGEESRIsLPLPNFsSLNLRETNLD SLNLRETNLDsLPLVDtHSKRTLLIKT	S49 S420 S39, S42 S412, S419 S430, T436
3	ZYX	AIsVSAPVFYAPQKK	S11	20.1	IPI00020513.2	Zyxin	APRPSPAISVsVSAPAFYAPQ	S73
4	RBM14	AQPSAsLGVGYR AQPSVsLGAPYR	S256 S280	3.1 19.4	IPI00013174.2	RNA binding motif protein 14	GAAYRAQPSAsLGVGYRTQPM AASYRAQPSVsLGAPYRGQLA	S256 S280
5	CNN2	AGQCVIGLQM*GtNK	T172	18.7	IPI00015262.10	calponin 2	GQCVIGLQMGtNKCASQSGMT	T172
6	-	LDLDLTADsQPPVFK	S416	18.3	IPI00438229.2	Tripartite motif-containing 28	ERLDLDLTADsQPPVFKVFPG	S501
7	CDV3	KAPQGPPEIYSDTQFPsLQSTAK	S197	18.2	IPI00014197.2	CDV3 homologue (mouse)	PEIYSDTQFPsLQSTAKHVES	S197
8	ARHGEF2	NNTALQSVsLR SVsTTNIAGHFNDEsPLGLR SVSTtNIAGHFNDEsPLGLR ILsQStDSLNMR	S109 S150, S162 T152, S162 S171, T174	17.7 8.1 5.8 6	IPI00291316.5	rho/rac guanine nucleotide exchange factor (GEF) 2	LKNNTALQSVsLRSKTTIRER RSSLSLAKSVsTTNIAGHFNDEsPLGLRRILSQ SLSLAKSVsTTNIAGHFNDEsPLGLRRILSQ ESPLGLRRILsQStDSLNMRNRTL	S109 S151, S163 T153, S163 S172, T175

[a] All events shown here have statistically significant induction. The complete list with all significant events and further details is shown in Supplemental Table 2. [b] Human IPI, Entrez name, and phosphosite are calculated by sequence alignment using Blast. [c] Phosphorylation at tyrosine, serine, or threonine is indicated by lower case "y", "s", or "t".
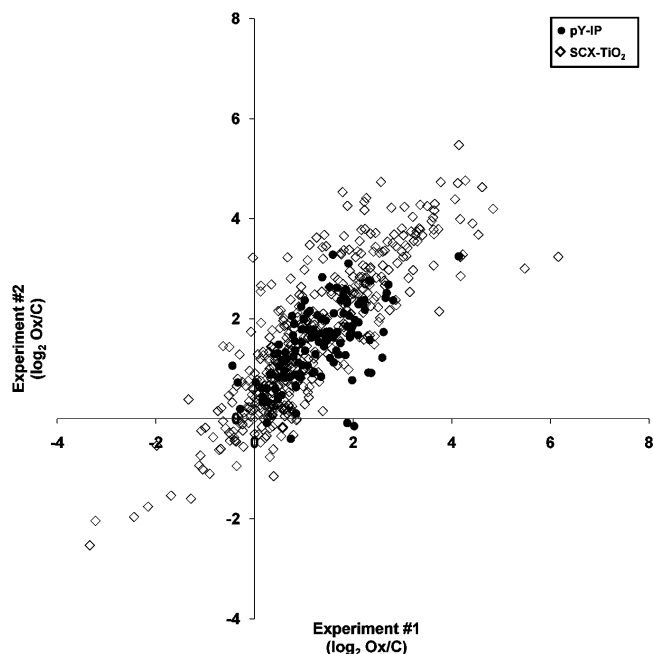
Figure 5. Reproducibility of quantitation measurements using phospho-peptide enrichment by phospho-tyrosine antibody (closed circle) and SCX-TiO$_2$ (open diamond). The ratio (log$_2$ Ox/C) was calculated for phosphopeptides found in two biological replicates.
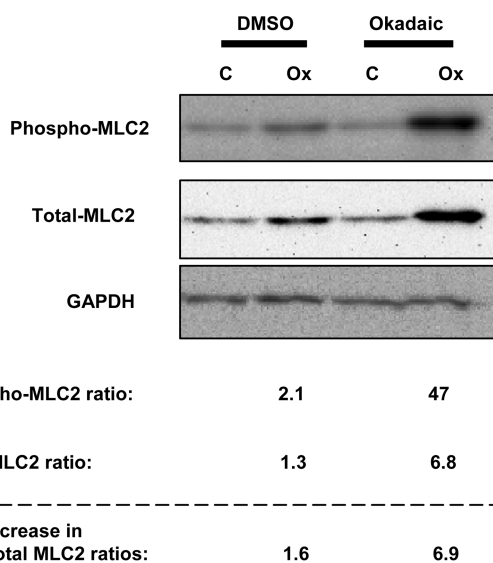

Figure 6. Ox-PAPC induces the phosphorylation of myosin light chain 2 (MLC2/MRLC2/MYL12B). BAECs were preincubated with, or without, 100 nM okadaic acid for 1 h before incubation with 40 μg/mL Ox-PAPC for 40 min. Immunoblots were probed for MLC2 phosphorylated at Thr18/Ser19 (top). The blot was then reprobed with an antibody to detect total levels of MLC2 (middle) and then for GAPDH (bottom). Numerical levels of phosphory-lated and unphosphorylated proteins were determined by quan-titative chemiluminescence and GAPDH levels were used to normalize each value for equal loading. The increase in phos-phorylation (phospho-MLC2/GAPDH) and protein levels (MLC2/GAPDH) induced by Ox-PAPC (Ox) are expressed as ratios compared to control cells treated with media alone (C). The fractional increase in phosphorylation per unit of MLC2 (phospho-MLC2/MLC2) between Control and Ox-PAPC is also indicated.

Another receptor tyrosine kinase that is phosphorylated upon Ox-PAPC exposure is TIE1, a receptor without a defined ligand.
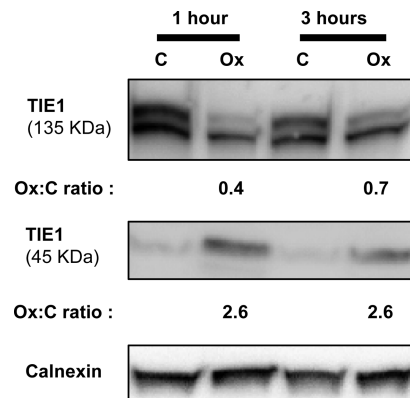
Figure 7. Ox-PAPC induces the cleavage of Tyrosine-protein kinase receptor TIE1 (TIE1). HAECs were incubated (in the absence of phosphatase inhibitors) with 40 μg/mL Ox-PAPC (Ox) or media alone (C) for different times. Cell lysates were analyzed by immunoblotting with anti-TIE1 antibody. Calnexin was used as a loading control. Ox-PAPC causes the cleavage of TIE1 reducing the size of this membrane protein from 135 to 45 kDa and releasing the extracellular part into the extracellular space. Ox-PAPC induced cleavage of TIE1 is potentially initiated by phosphorylation of the receptor based on the increases in phosphorylation observed by mass spectrometry (Supplemental Table 1) and previous reports in which phosphorylation induced by other stimuli leads to cleavage.[46] The decrease in 135 kDa TIE1 and the increase in 45 kDa TIE1 induced by Ox-PAPC were determined by quantitative chemiluminescence and expressed as fold increase compared to cells treated with media alone (Ox:C ratio).

Table 3. Partial List of KEGG Pathways and GO Terms Enriched in the Lists of Phosphoproteins Modulated by Ox-PAPC Stimulation[a]

KEGG pathway	p-value[b]
hsa04810:Regulation of actin cytoskeleton	0.017
hsa04520:Adherens junction	0.12
hsa04370:VEGF signaling pathway	0.15
hsa04510:Focal adhesion	0.16
hsa04012:ErbB signaling pathway	0.16

GO term	p-value[b]
GO:0005856 cytoskeleton	3.0×10^{-6}
GO:0006928 cell motility	6.3×10^{-3}
GO:0005886 plasma membrane	8.4×10^{-3}
GO:0004672 protein kinase activity	0.032
GO:0005543 phospholipid binding	0.034
GO:0005083 small GTPase regulator activity	0.053

[a] The complete list is shown in Supplemental Tables 3 and 4. [b] Enrichment p-values were calculated using the phosphoproteins with statistically significant Ox-PAPC-induced changes in phosphorylation as the gene list and the phosphorylated proteins detected in this study as the background reference set (Methods). Additional pathway enrichment analysis was also done to compare the types of phosphorylated proteins detected in aortic endothelial cells compared to all proteins encoded in the genome. This analysis is fully described in Supplemental Tables 3 and 4 along with additional results.

The phosphorylation of TIE1 induced by other endothelial cell activators such as PMA, VEGF, or shear stress is associated with the cleavage of the receptor.[46,47] The cleavage of TIE1 is important in regulating the activation of the family member TIE2 by angiopoietins[46] and leads to vascular remodeling.[48] In our validation studies, we found that Ox-PAPC causes the cleavage of TIE1 in HAECs (Figure 7). This suggests a new

Table 4. Phosphoproteins with Ox-PAPC-Induced Phosphorylation That Are Involved in the Regulation of Actin Cytoskeleton (KEGG Pathway hsa04810)

protein	Entrez	phosphorylation site induced by Ox-PAPC. Bovine site (Human site)[a]	reported activation by Ox-PAPC[b]
PAXILLIN	PXN	S302 (S272)	Phosphosites reported[32] Y31, Y118, S126, S178, S272
INTEGRIN, BETA 1	ITGB1	Y783 (Y783)	Yes, but no phosphosite identified[34]
MYOSIN LIGHT CHAIN 2	MLC2/MRLC2/ MYL12B	T18 (T19) S19 (S20)	Reported no change of this site upon induction by Ox-PAPC[12]
INTEGRIN, BETA 4	ITGB4	S1060 (S1069) S1442 (S1454) S1445 (S1457)	
MYOSIN, HEAVY POLYPEPTIDE 10, NON-MUSCLE	MYH10	S641 (S641) S1939 (S1939)	
THYMOSIN, BETA 4, X-LINKED	TMSB4X	T34 (T53)	
P21 (CDKN1A)-ACTIVATED KINASE 2	PAK2	S5 (S197)	Phosphosite reported in PAK1[32] T423
INTEGRIN, BETA 3	ITGB3	Y781 (Y785)	
MITOGEN-ACTIVATED PROTEIN KINASE 1	MAPK1	Y187 (Y187)	Phosphosite reported[9,31] T185, Y187
MITOGEN-ACTIVATED PROTEIN KINASE 3	MAPK3	T185 (T202) Y187 (Y204)	Phosphosite reported[9,31] T202, Y204
ACTIN, BETA	ACTB	Y169 (Y169)	Yes, but no phosphosite identified[40]
ACTIN RELATED PROTEIN 2/3 COMPLEX, SUBUNIT 1B, 41KDA	ARPC1B	S323 (S323)	
WISKOTT-Aldrich SYNDROME-LIKE	WASL	Y256 (Y256)	
ACTININ, ALPHA 1	ACTN1	Y246 (Y246)	
BREAST CANCER ANTI-ESTROGEN RESISTANCE 1	BCAR1	T530 (T600)	
VINCULIN	VCL	S290 (S290) Y497 (Y822)	Yes, but no phosphosite identified[41]

[a] Phosphosite induction by Ox-PAPC observed in this study. [b] Previously reported phosphosite inductions by Ox-PAPC.

mechanism of endothelial cell activation regulated by Ox-PAPC where the oxidized phospholipid causes the cleavage of TIE1 and thus allows for a stronger activation of TIE2 by angiopoietins. While the association between phosphorylation of TIE1 and cleavage of the receptor was known previously, the phosphorylation site that mediates this effect was not known. The site reported here (Tyr1083 in human) is thus a candidate for future mechanistic studies.

Conclusion

To our knowledge, this is the first phospho-proteomic study with oxidized phospholipids as cell activators. We applied phospho-profiling to primary cell culture rather than to cell lines to better represent signaling events taking place in the endothelium in vivo. The overlap of our results with previous findings demonstrates that use of bovine aortic endothelial cells, which are available in the large numbers needed for shotgun proteomics, can provide results of relevance to human

endothelial cells. One major difference between the shotgun phosphoproteomic analysis methods used here and other studies is the application of solid-phase extraction cartridges, instead of HPLC, to separate peptides by SCX. This simplifies and economizes sample preparation but may also reduce the number of phosphopeptides that can be identified.

The goal of this study was to identify changes in protein phosphorylation and thus signal transduction induced by Ox-PAPC in aortic endothelial cells, and determine the sites where this modification occurs. In the course of optimization, we added phosphatase inhibitors to prevent transient events from returning to their basal phosphorylation and to facilitate phosphorylation event identification by phosphopeptide enrichment and mass spectrometry. The use of phosphatase inhibitors could artificially result in phosphorylation event inductions not seen in the absence of inhibitors, or could alter the magnitude of phosphorylation event inductions. However, we demonstrated that distinct patterns of phosphorylation

Table 5. Phosphoproteins with Ox-PAPC-Induced Phosphorylation That Are Annotated As Having Protein Kinase Activity (GO:0004672)

protein	Entrez	phosphorylation site induced by Ox-PAPC. Bovine site (Human site)[a]	reported activation by Ox-PAPC[b]
PROTEIN KINASE N2	PKN2	S21 (S21)	
MISSHAPEN-LIKE KINASE 1	MINK1	S728 (S729) S742 (S743)	
TYROSINE KINASE, NON-RECEPTOR, 2	TNK2	Y858 (Y913)	
MITOGEN-ACTIVATED PROTEIN KINASE 7	MAPK7	Y221 (Y221)	
MITOGEN-ACTIVATED PROTEIN KINASE KINASE KINASE 11	MAP3K11	S524 (S524)	
P21 PROTEIN (CDC42/RAC)-ACTIVATED KINASE 2	PAK2	S5 (S197)	Phosphosite reported in PAK1[32] T423
MAP/MICROTUBULE AFFINITY-REGULATING KINASE 3	MARK3	S409 (S540) S412 (S543)	
PROTEIN KINASE N1	PKN1	S924 (S922)	
MITOGEN-ACTIVATED PROTEIN KINASE 1	MAPK1	Y187 (Y187)	Phosphosite reported[9,31] T185, Y187
MITOGEN-ACTIVATED PROTEIN KINASE 3	MAPK3	T185 (T202) Y187 (Y204)	Phosphosite reported[9,31] T202, Y204
MITOGEN-ACTIVATED PROTEIN KINASE KINASE KINASE KINASE 4	MAP4K4	S730 (S773) S741 (S784)	
EPH RECEPTOR A2	EPHA2	T593 (T593) Y594 (Y594) Y771 (Y772) T773 (T774)	
TYROSINE KINASE WITH IMMUNOGLOBULIN-LIKE AND EGF-LIKE DOMAINS 1	TIE1	Y1084 (Y1083)	
AP2 ASSOCIATED KINASE 1	AAK1	S782 (gap)	
NKF3 KINASE FAMILY MEMBER	SGK269	T615 (T615) Y635 (Y635)	
EPH RECEPTOR A5	EPHA5	T355 (T812)	
JANUS KINASE 2	JAK2	Y570 (Y570)	Phosphosite reported[8] Y1007, Y1008
PRP4 PRE-MRNA PROCESSING FACTOR 4 HOMOLOGUE B	PRPF4B	Y850 (Y849)	
GENERAL TRANSCRIPTION FACTOR IIF, POLYPEPTIDE 1	GTF2F1	S385 (S385) T389 (T389)	
KINASE INSERT DOMAIN RECEPTOR	KDR/VEGFR2	Y1214 (Y1214)	Phosphosite reported[31] Y1175
CYCLIN-DEPENDENT KINASE 2	CDK2	T14 (T14) Y15 (Y15)	
TYROSINE KINASE 2	TYK2	Y293 (Y292)	
GLYCOGEN SYNTHASE KINASE 3 BETA	GSK3B	Y216 (Y216)	
BMX NON-RECEPTOR TYROSINE KINASE	BMX	Y212 (Y234) Y344 (Y365)	
DUAL-SPECIFICITY TYROSINE-(Y)-PHOSPHORYLATION REGULATED KINASE 1A	DYRK1A	Y312 (Y312)	

[a] Phosphosite induction by Ox-PAPC observed in this study. [b] Previously reported phosphosite inductions by Ox-PAPC.

induced by Ox-PAPC, VEGF, and TNF-α are observed even in the presence of the phosphatase inhibitors vanadate and okadaic acid (Figure 1). These differences indicate that the phosphatase inhibitors do not overwhelm pathway-specific regulation of signal transduction pathways. Furthermore, we have demonstrated that many phosphorylated proteins identified in the present study were also previously identified as phosphorylated, using immunoblotting-based analysis, in cells exposed to Ox-PAPC in the absence of inhibitors (Tables 4 and 5). Finally, several of the proteins we identified as being

phosphorylated have been shown to play an important role in Ox-PAPC action. Also, we identified candidate phosphorylation sites on a number of proteins that have been demonstrated in previously published studies to be activated after treatment with Ox-PAPC, but where the previous studies had not identified the site of phosphorylation. VEGFR2 activation is important in the inflammatory and pro-coagulant responses to Ox-PAPC.[31] VE-Cadherin phosphorylation and MLC2 phosphorylation will be shown in a forthcoming publication to be important in the increased permeability of the endothelial monolayer in response to higher but subtoxic concentrations of Ox-PAPC. Thus, our studies provide evidence that use of phosphatase inhibitors can aid in the identification of proteins phosphorylated by treatment of cells with Ox-PAPC. However, it remains important to validate any identification reported here with independent testing of activation in cell biology studies in the absence of inhibitors.

In summary, the list of phosphorylation events induced by Ox-PAPC provides many candidate regulators of Ox-PAPC action. Furthermore, our studies identify the specific phosphorylation sites that could modulate this action. As a group, these results point to signaling events that are involved in the initiation of Ox-PAPC-induced activation of endothelial cells (receptor tyrosine kinases) and may influence the phenotypes associated with atherosclerosis such as maintenance, breakdown and infiltration of the endothelial barrier. These system-wide findings provide guidance to better understand the network of signaling events controlling the profound and unique activation of endothelial cells by Ox-PAPC, a molecule implicated in the pathogenesis of atherosclerosis.

Supporting Information Available: Tables listing the quantitation of phosphopeptides isolated from Control and Ox-PAPC treated cells using a pan-specific anti-phosphotyrosine antibody, and using fractionation of peptides by SCX followed by enrichment of phosphopeptides by TiO_2 metal affinity, complete lists of KEGG pathways and GO terms enriched in the lists of phosphoproteins modulated by Ox-PAPC stimulation, or enriched in the lists of phosphoproteins detected in aortic endothelial cells, and phosphoproteins with Ox-PAPC-induced phosphorylation levels that are involved in focal adhesion. Figures of mass spectrometry alignment and quantitation analysis pipeline, distribution of phosphopeptides in the SCX chromatography fractions based on their solution charge state at pH 2.7, percentage of phosphopeptides present in each fraction after separation by SCX chromatography and enrichment of phosphopeptides using TiO_2 metal affinity, distribution of phosphopeptides based on the number of phosphate groups found after enrichment of phosphopeptides by SCX-TiO_2, and determination of significant phosphorylation changes induced by Ox- PAPC based on ratio and *t*-test *p*-value comparisons between different and like samples. This material is available free of charge via the Internet at http://pubs.acs.org.

References

(1) Leitinger, N.; Tyner, T. R.; Oslund, L.; Rizza, C.; Subbanagounder, G.; Lee, H.; Shih, P. T.; Mackman, N.; Tigyi, G.; Territo, M. C.; Berliner, J. A.; Vora, D. K. Structurally similar oxidized phospholipids differentially regulate endothelial binding of monocytes and neutrophils. *Proc. Natl. Acad. Sci. U.S.A.* **1999**, *96* (21), 12010–5.

(2) Chang, M. K.; Binder, C. J.; Miller, Y. I.; Subbanagounder, G.; Silverman, G. J.; Berliner, J. A.; Witztum, J. L. Apoptotic cells with oxidation-specific epitopes are immunogenic and proinflammatory. *J. Exp. Med.* **2004**, *200* (11), 1359–70.

(3) Watson, A. D.; Leitinger, N.; Navab, M.; Faull, K. F.; Horkko, S.; Witztum, J. L.; Palinski, W.; Schwenke, D.; Salomon, R. G.; Sha, W.; Subbanagounder, G.; Fogelman, A. M.; Berliner, J. A. Structural identification by mass spectrometry of oxidized phospholipids in minimally oxidized low density lipoprotein that induce monocyte/endothelial interactions and evidence for their presence in vivo. *J. Biol. Chem.* **1997**, *272* (21), 13597–607.

(4) Tsimikas, S.; Brilakis, E. S.; Miller, E. R.; McConnell, J. P.; Lennon, R. J.; Kornman, K. S.; Witztum, J. L.; Berger, P. B. Oxidized phospholipids, Lp(a) lipoprotein, and coronary artery disease. *N. Engl. J. Med.* **2005**, *353* (1), 46–57.

(5) Berliner, J. A.; Watson, A. D. A role for oxidized phospholipids in atherosclerosis. *N. Engl. J. Med.* **2005**, *353* (1), 9–11.

(6) Gargalovic, P. S.; Imura, M.; Zhang, B.; Gharavi, N. M.; Clark, M. J.; Pagnon, J.; Yang, W. P.; He, A.; Truong, A.; Patel, S.; Nelson, S. F.; Horvath, S.; Berliner, J. A.; Kirchgessner, T. G.; Lusis, A. J. Identification of inflammatory gene modules based on variations of human endothelial cell responses to oxidized lipids. *Proc. Natl. Acad. Sci. U.S.A.* **2006**, *103* (34), 12741–6.

(7) Yeh, M.; Leitinger, N.; de Martin, R.; Onai, N.; Matsushima, K.; Vora, D. K.; Berliner, J. A.; Reddy, S. T. Increased transcription of IL-8 in endothelial cells is differentially regulated by TNF-alpha and oxidized phospholipids. *Arterioscler., Thromb., Vasc. Biol.* **2001**, *21* (10), 1585–91.

(8) Gharavi, N. M.; Alva, J. A.; Mouillesseaux, K. P.; Lai, C.; Yeh, M.; Yeung, W.; Johnson, J.; Szeto, W. L.; Hong, L.; Fishbein, M.; Wei, L.; Pfeffer, L. M.; Berliner, J. A. Role of the Jak/STAT pathway in the regulation of interleukin-8 transcription by oxidized phospholipids in vitro and in atherosclerosis in vivo. *J. Biol. Chem.* **2007**, *282* (43), 31460–8.

(9) Bochkov, V. N.; Mechtcheriakova, D.; Lucerna, M.; Huber, J.; Malli, R.; Graier, W. F.; Hofer, E.; Binder, B. R.; Leitinger, N. Oxidized phospholipids stimulate tissue factor expression in human endothelial cells via activation of ERK/EGR-1 and Ca(++)/NFAT. *Blood* **2002**, *99* (1), 199–206.

(10) Yeh, M.; Gharavi, N. M.; Choi, J.; Hsieh, X.; Reed, E.; Mouillesseaux, K. P.; Cole, A. L.; Reddy, S. T.; Berliner, J. A. Oxidized phospholipids increase interleukin 8 (IL-8) synthesis by activation of the c-src/signal transducers and activators of transcription (STAT)3 pathway. *J. Biol. Chem.* **2004**, *279* (29), 30175–81.

(11) Gharavi, N. M.; Baker, N. A.; Mouillesseaux, K. P.; Yeung, W.; Honda, H. M.; Hsieh, X.; Yeh, M.; Smart, E. J.; Berliner, J. A. Role of endothelial nitric oxide synthase in the regulation of SREBP activation by oxidized phospholipids. *Circ. Res.* **2006**, *98* (6), 768–76.

(12) Birukov, K. G.; Leitinger, N.; Bochkov, V. N.; Garcia, J. G. Signal transduction pathways activated in human pulmonary endothelial cells by OxPAPC, a bioactive component of oxidized lipoproteins. *Microvasc. Res.* **2004**, *67* (1), 18–28.

(13) Rush, J.; Moritz, A.; Lee, K. A.; Guo, A.; Goss, V. L.; Spek, E. J.; Zhang, H.; Zha, X. M.; Polakiewicz, R. D.; Comb, M. J. Immunoaffinity profiling of tyrosine phosphorylation in cancer cells. *Nat. Biotechnol.* **2005**, *23* (1), 94–101.

(14) Olsen, J. V.; Blagoev, B.; Gnad, F.; Macek, B.; Kumar, C.; Mortensen, P.; Mann, M. Global, in vivo, and site-specific phosphorylation dynamics in signaling networks. *Cell* **2006**, *127* (3), 635–48.

(15) Villen, J.; Beausoleil, S. A.; Gerber, S. A.; Gygi, S. P. Large-scale phosphorylation analysis of mouse liver. *Proc. Natl. Acad. Sci. U.S.A.* **2007**, *104* (5), 1488–93.

(16) Skaggs, B. J.; Gorre, M. E.; Ryvkin, A.; Burgess, M. R.; Xie, Y.; Han, Y.; Komisopoulou, E.; Brown, L. M.; Loo, J. A.; Landaw, E. M.; Sawyers, C. L.; Graeber, T. G. Phosphorylation of the ATP-binding loop directs oncogenicity of drug-resistant BCR-ABL mutants. *Proc. Natl. Acad. Sci. U.S.A.* **2006**, *103* (51), 19466–71.

(17) Lee, S.; Chen, T. T.; Barber, C. L.; Jordan, M. C.; Murdock, J.; Desai, S.; Ferrara, N.; Nagy, A.; Roos, K. P.; Iruela-Arispe, M. L. Autocrine VEGF signaling is required for vascular homeostasis. *Cell* **2007**, *130* (4), 691–703.

(18) Natarajan, V.; Scribner, W. M.; Vepa, S. Phosphatase inhibitors potentiate 4-hydroxynonenal-induced phospholipase D activation in vascular endothelial cells. *Am. J. Respir. Cell Mol. Biol.* **1997**, *17* (2), 251–9.

(19) Chang, N. T.; Huang, L. E.; Liu, A. Y. Okadaic acid markedly potentiates the heat-induced hsp 70 promoter activity. *J. Biol. Chem.* **1993**, *268* (2), 1436–9.

(20) Boeri Erba, E.; Matthiesen, R.; Bunkenborg, J.; Schulze, W. X.; Di Stefano, P.; Cabodi, S.; Tarone, G.; Defilippi, P.; Jensen, O. N. Quantitation of multisite EGF receptor phosphorylation using mass spectrometry and a novel normalization approach. *J. Proteome Res.* **2007**, *6* (7), 2768–85.

(21) Sugiyama, N.; Masuda, T.; Shinoda, K.; Nakamura, A.; Tomita, M.; Ishihama, Y. Phosphopeptide enrichment by aliphatic hydroxy acid-modified metal oxide chromatography for nano-LC-MS/MS in proteomics applications. *Mol. Cell. Proteomics* **2007**, *6* (6), 1103–9.

(22) Beausoleil, S. A.; Villen, J.; Gerber, S. A.; Rush, J.; Gygi, S. P. A probability-based approach for high-throughput protein phosphorylation analysis and site localization. *Nat. Biotechnol.* **2006**, *24* (10), 1285–92.

(23) Prakash, A.; Mallick, P.; Whiteaker, J.; Zhang, H.; Paulovich, A.; Flory, M.; Lee, H.; Aebersold, R.; Schwikowski, B. Signal maps for mass spectrometry-based comparative proteomics. *Mol. Cell. Proteomics* **2006**, *5* (3), 423–32.

(24) Andreev, V. P.; Li, L.; Cao, L.; Gu, Y.; Rejtar, T.; Wu, S. L.; Karger, B. L. A new algorithm using cross-assignment for label-free quantitation with LC-LTQ-FT MS. *J. Proteome Res.* **2007**, *6* (6), 2186–94.

(25) Jaitly, N.; Monroe, M. E.; Petyuk, V. A.; Clauss, T. R.; Adkins, J. N.; Smith, R. D. Robust algorithm for alignment of liquid chromatography-mass spectrometry analyses in an accurate mass and time tag data analysis pipeline. *Anal. Chem.* **2006**, *78* (21), 7397–409.

(26) Ono, M.; Shitashige, M.; Honda, K.; Isobe, T.; Kuwabara, H.; Matsuzuki, H.; Hirohashi, S.; Yamada, T. Label-free quantitative proteomics using large peptide data sets generated by nanoflow liquid chromatography and mass spectrometry. *Mol. Cell. Proteomics* **2006**, *5* (7), 1338–47.

(27) Prince, J. T.; Marcotte, E. M. Chromatographic alignment of ESI-LC-MS proteomics data sets by ordered bijective interpolated warping. *Anal. Chem.* **2006**, *78* (17), 6140–52.

(28) Sadygov, R. G.; Maroto, F. M.; Huhmer, A. F. ChromAlign: A two-step algorithmic procedure for time alignment of three-dimensional LC-MS chromatographic surfaces. *Anal. Chem.* **2006**, *78* (24), 8207–17.

(29) Dennis, G., Jr.; Sherman, B. T.; Hosack, D. A.; Yang, J.; Gao, W.; Lane, H. C.; Lempicki, R. A. DAVID: Database for Annotation, Visualization, and Integrated Discovery. *Genome Biol.* **2003**, *4* (5), P3.

(30) Villen, J.; Gygi, S. P. The SCX/IMAC enrichment approach for global phosphorylation analysis by mass spectrometry. *Nat. Protoc.* **2008**, *3* (10), 1630–8.

(31) Zimman, A.; Mouillesseaux, K. P.; Le, T.; Gharavi, N. M.; Ryvkin, A.; Graeber, T. G.; Chen, T. T.; Watson, A. D.; Berliner, J. A. Vascular endothelial growth factor receptor 2 plays a role in the activation of aortic endothelial cells by oxidized phospholipids. *Arterioscler., Thromb., Vasc. Biol.* **2007**, *27* (2), 332–8.

(32) Birukova, A. A.; Alekseeva, E.; Cokic, I.; Turner, C. E.; Birukov, K. G. Cross talk between paxillin and Rac is critical for mediation of barrier-protective effects by oxidized phospholipids. *Am. J. Physiol.: Lung Cell. Mol. Physiol.* **2008**, *295* (4), L593–602.

(33) Singleton, P. A.; Chatchavalvanich, S.; Fu, P.; Xing, J.; Birukova, A. A.; Fortune, J. A.; Klibanov, A. M.; Garcia, J. G.; Birukov, K. G.

Akt-mediated transactivation of the S1P1 receptor in caveolin-enriched microdomains regulates endothelial barrier enhancement by oxidized phospholipids. *Circ. Res.* **2009**, *104* (8), 978–86.

(34) Shih, P. T.; Elices, M. J.; Fang, Z. T.; Ugarova, T. P.; Strahl, D.; Territo, M. C.; Frank, J. S.; Kovach, N. L.; Cabanas, C.; Berliner, J. A.; Vora, D. K. Minimally modified low-density lipoprotein induces monocyte adhesion to endothelial connecting segment-1 by activating beta1 integrin. *J. Clin. Invest.* **1999**, *103* (5), 613–25.

(35) Legate, K. R.; Fassler, R. Mechanisms that regulate adaptor binding to beta-integrin cytoplasmic tails. *J. Cell Sci.* **2009**, *122* (Pt. 2), 187–98.

(36) Cole, A. L.; Subbanagounder, G.; Mukhopadhyay, S.; Berliner, J. A.; Vora, D. K. Oxidized phospholipid-induced endothelial cell/monocyte interaction is mediated by a cAMP-dependent R-Ras/PI3-kinase pathway. *Arterioscler., Thromb., Vasc. Biol.* **2003**, *23* (8), 1384–90.

(37) Lee, S.; Gharavi, N. M.; Honda, H.; Chang, I.; Kim, B.; Jen, N.; Li, R.; Zimman, A.; Berliner, J. A. A role for NADPH oxidase 4 in the activation of vascular endothelial cells by oxidized phospholipids. *Free Radical Biol. Med.* **2009**, *47* (2), 145–51.

(38) Liu, Y.; Sweet, D. T.; Irani-Tehrani, M.; Maeda, N.; Tzima, E. Shc coordinates signals from intercellular junctions and integrins to regulate flow-induced inflammation. *J. Cell Biol.* **2008**, *182* (1), 185–96.

(39) Lee, J. S.; Gotlieb, A. I. Understanding the role of the cytoskeleton in the complex regulation of the endothelial repair. *Histol. Histopathol.* **2003**, *18* (3), 879–87.

(40) Birukova, A. A.; Fu, P.; Chatchavalvanich, S.; Burdette, D.; Oskolkova, O.; Bochkov, V. N.; Birukov, K. G. Polar head groups are important for barrier-protective effects of oxidized phospholipids on pulmonary endothelium. *Am. J. Physiol.: Lung Cell. Mol. Physiol.* **2007**, *292* (4), L924–35.

(41) Birukova, A. A.; Malyukova, I.; Poroyko, V.; Birukov, K. G. Paxillin-beta-catenin interactions are involved in Rac/Cdc42-mediated endothelial barrier-protective response to oxidized phospholipids. *Am. J. Physiol.: Lung Cell. Mol. Physiol.* **2007**, *293* (1), L199–211.

(42) Han, J.; Liu, G.; Profirovic, J.; Niu, J.; Voyno-Yasenetskaya, T., Zyxin is involved in thrombin signaling via interaction with PAR-1 receptor. *Faseb J* 2009.

(43) Nikolopoulos, S. N.; Blaikie, P.; Yoshioka, T.; Guo, W.; Giancotti, F. G. Integrin beta4 signaling promotes tumor angiogenesis. *Cancer Cell* **2004**, *6* (5), 471–83.

(44) Li, R.; Mouillesseaux, K. P.; Montoya, D.; Cruz, D.; Gharavi, N.; Dun, M.; Koroniak, L.; Berliner, J. A. Identification of prostaglandin E2 receptor subtype 2 as a receptor activated by OxPAPC. *Circ. Res.* **2006**, *98* (5), 642–50.

(45) Olsson, A. K.; Dimberg, A.; Kreuger, J.; Claesson-Welsh, L. VEGF receptor signalling—in control of vascular function. *Nat. Rev. Mol. Cell Biol.* **2006**, *7* (5), 359–71.

(46) Marron, M. B.; Singh, H.; Tahir, T. A.; Kavumkal, J.; Kim, H. Z.; Koh, G. Y.; Brindle, N. P. Regulated proteolytic processing of Tie1 modulates ligand responsiveness of the receptor-tyrosine kinase Tie2. *J. Biol. Chem.* **2007**, *282* (42), 30509–17.

(47) Chen-Konak, L.; Guetta-Shubin, Y.; Yahav, H.; Shay-Salit, A.; Zilberman, M.; Binah, O.; Resnick, N. Transcriptional and post-translation regulation of the Tie1 receptor by fluid shear stress changes in vascular endothelial cells. *FASEB J.* **2003**, *17* (14), 2121–3.

(48) Eklund, L.; Olsen, B. R. Tie receptors and their angiopoietin ligands are context-dependent regulators of vascular remodeling. *Exp. Cell Res.* **2006**, *312* (5), 630–41.

PR901194X